ELSEVIER

Signal Processing 42 (1995) 273–289

SIGNAL PROCESSING

Multiband signal reconstruction from finite samples☆

Xiang-Gen Xia[a,*,1], C.-C. Jay Kuo[b], Zhen Zhang[c]

[a]*Department of Electrical and Computer Engineering, Air Force Institute of Technology, Wright-Patterson AFB, OH 45433-7765, USA*
[b]*Department of Electrical Engineering-Systems, Signal and Image Processing Institute, University of Southern California, Los Angeles, CA 90089-2564, USA*
[c]*Department of Electrical Engineering-Systems, Communication Sciences Institute, University of Southern California, Los Angeles, CA 90089-2565, USA*

Received 28 February 1994; revised 13 October 1994

Abstract

The minimum mean-squared error (MMSE) estimator has been used to reconstruct a band-limited signal from its finite samples in a bounded interval and shown to have many nice properties. In this research, we consider a special class of band-limited 1-D and 2-D signals which have a multiband structure in the frequency domain, and propose a new reconstruction algorithm to exploit the multiband feature of the underlying signals. The concept of the critical value and region is introduced to measure the performance of a reconstruction algorithm. We show analytically that the new algorithm performs better than the MMSE estimator for band-limited/multiband signals in terms of the critical value and region measure. Finally, numerical examples of 1-D and 2-D signal reconstruction are given for performance comparison of various methods.

Zusammenfassung

Der Minimum-Mean-Squared-Error-(MMSE) Schätzer wurde zur Rekonstruktion eines bandbegrenzten Signals aus endlich vielen Abtastwerten aus einem begrenzten Intervall benutzt und es zeigt sich, daß er viele günstige Eigenschaften aufweist. In dieser Arbeit betrachten wir eine spezielle Klasse bandbegrenzter 1D- und 2D-Signale mit Multiband-Struktur im Frequenzbereich und schlagen einen neuen Rekonstruktionsalgorithmus vor, der die Multiband-Eigenschaft des zugrundeliegenden Signals ausnutzt. Zur Bewertung des Rekonstruktionsalgorithmus wird das Konzept des kritischen Wertes und Gebietes eingeführt. Wir zeigen analytisch, daß der neue Algorithmus besser arbeitet als der MMSE-Schätzer für bandbegrenzte/Multiband-Signale in Abhängigkeit vom kritischen Wert und Gebiets-Maß, Schließlich werden numerische Beispiele zur Rekonstruktion von 1D- und 2D-Signalen gegeben, wobei die Eigenschaften verschiedener Methoden verglichen werden.

Résumé

L'estimateur de l'erreur minimale au sens des moindres carrés (EMMC) a été utilisé pour reconstruire un signal a bande limitée à partir de ses échantillons finis sur un intervalle fermé, et a montré qu'il avait des propriétés intéressantes.

☆This work was supported by the National Science Foundation Grant NCR-9205265, the National Science Foundation Young Investigator (NYI) Award ASC-9258396 and the Presidential Faculty Fellow (PFF) Award GER 93-50309.

*Corresponding author.

[1]He was with Communication Sciences Institute, Department of Electrical Engineering-Systems, University of Southern California, Los Angeles, CA 90089-2565, USA.

SSDI 0165-1684(94)00135-9

Dans ce travail, nous considérons une classe particulière, de signaux à bande limitée 1D et 2D, qui ont une structure multi-bande dans le domaine fréquenciel; nous proposons un nouvel algorithme de réconstruction pour exploiter la caractéristique multi-bande des signaux sous-jacents. Le concept de region et de valeur critiques est introduit, dans le but de mesurer les performances d'un algorithme de réconstruction. Nous montrons analytiquement que le nouvel algorithme se comporte mieux que l'estimateur EMMC pour les signaux à bande limitée/multi-bande en termes de mesure des region et valeur critiques. Enfin, des exemples numériques de reconstruction de signaux 1D et 2D sont donnés pour comparer les performances de plusieurs méthodes.

Keywords: MMSE; Multiband signals; Extrapolation; Sampling; Critical value and region

1. Introduction

Band-limited signal reconstruction from observed samples in a bounded interval is important in many signal processing and communication applications. It has been extensively studied by many researchers, say, [2–12, 16–21, 25–32, 36–40], and from prediction point of view, [24, 23, 3]. This problem can be generally stated as: given a band-limited signal $f(t)$ with bandwidth Ω, i.e. $\hat{f}(\omega) = 0$ for $|\omega| > \Omega$, we want to recover the signal $f(t)$ from a limited number of samples $f(t_i)$, $i = 1, 2, \ldots, N$. The performance of existing reconstruction methods usually depends on the bandwidth Ω of $f(t)$. That is, algorithms perform poorer when the bandwidth Ω becomes larger. However, in some applications the spectrum of the signal $f(t)$ does not fill the whole bandwidth $[-\Omega, \Omega]$ but was a multi-band structure in $[-\Omega, \Omega]$ as shown in Fig. 1. One such example is signal transmission via frequency modulation with several carrier frequencies. Then, it is natural to seek an effective algorithm which reconstructs the signal by taking advantage of the multiband feature.

The multiband signal sampling problem has been recently addressed by Vaughan et al. [34] and Beaty and Dodson [1]. An interesting result obtained is that it is possible to uniformly sample a multiband signal with a rate lower than the Nyquist rate based on the bandwidth Ω for its perfect reconstruction. Most recently Ries in [28] studied the reconstruction problem of real and analytic band-pass signals from a finite number of samples based on the truncations of the sampling theorems. Since the sampling theorems basically require that the sample points spread on the whole time domain with certain distance between adjacent sample points which should not be too large.

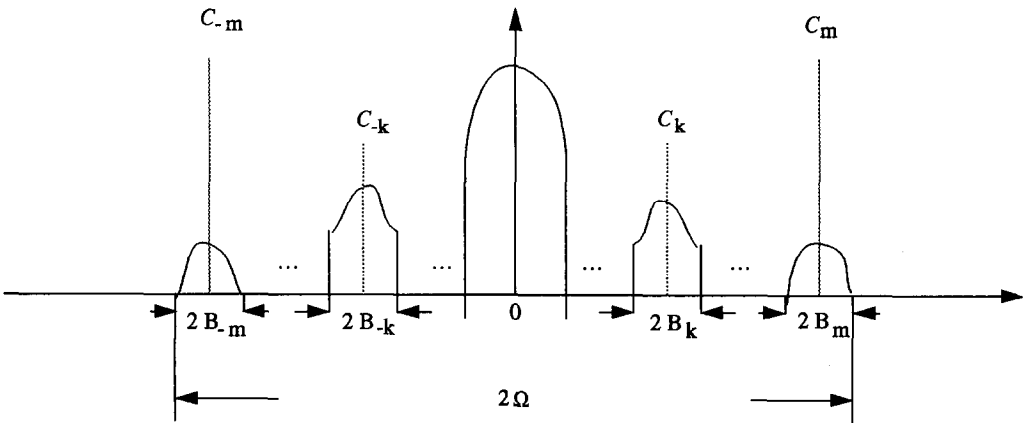

Fig. 1. Fourier spectrum of a multiband signal.

Therefore, to have a good reconstruction an observation in a large time interval is usually needed, which may not be satisfied in some applications. The following reconstruction problem is studied in this research. Let $f(t)$ be a multiband signal with its Fourier spectrum as shown in Fig. 1, where we assume that the bandwidth B_k and the center position C_k of each band indexed by $-m \leqslant k \leqslant m$ are known. Now, given a finite known samples $f(t_i)$, $t_i \in [-T, T]$ for an arbitrarily fixed $T > 0$, $i = 1, 2, \ldots, m$, we want to find an approximation $\tilde{f}(t)$ of $f(t)$ with $t \in [-\tau, \tau]$, where $\tau \geqslant T$. Multiband signal reconstructions from finite samples occur in many applications, for example, optics [10], radar [15], sonar [13], communications [35], biomedical signals [8] and power measurement [7].

In this work, we propose a new reconstruction algorithm for the above problem, which is *not* motivated from the sampling theorems but from signal extrapolations where the length of the observation time interval may be arbitrary. To measure the performance of different methods, we introduce the concept of the critical region and the critical value. Roughly speaking, by the critical region, we mean the area that the reconstructed signal $\tilde{f}(t)$ provides a good approximation of the true signal $f(t)$. Then, we use the critical value to characterize the length or the area of the critical region for 1-D and 2-D signals, respectively. We obtain an explicit expression for the critical value of the new algorithm, and show that it is better than the minimum mean-squared error (MMSE) estimator where the multiband structure is not exploited. For modulated real signals, we can improve the reconstruction method further so that its critical value is almost twice as large as the one applicable to general complex multiband signals with Fourier spectrum shown in Fig. 1. We also consider the extension of the new algorithm to 2-D multiband signals which has applications in image processing. Numerical examples in both 1-D and 2-D cases are given for performance comparison of various methods.

This paper is organized as follows. The MMSE estimator for band-limited signal reconstruction is briefly reviewed, and the concept of the critical value and region is introduced in Section 2. We study the 1-D and 2-D multiband signal reconstruction problems in Sections 3 and 4, respectively. We use some numerical examples to demonstrate the performance of the proposed algorithm in Section 5, and concluding remarks are given in Section 6.

2. Critical regions and values for band-limited signal reconstruction

This section reviews some basic results of band-limited signal reconstruction [6, 18, 21, 36]. The main objective is to introduce the concept of critical region and its associated critical value for a given interpolant. We will examine both 1-D and 2-D cases.

Let $f(t)$ be an Ω band-limited signal and $f(t_i)$, $i = 1, 2, \ldots, m$, be given samples of $f(t)$. Then, the MMSE estimator for $f(t)$ is of the form (see [6])

$$\Phi_m(t) = \sum_{k=1}^{m} a_k \frac{\sin \Omega(t - t_k)}{t - t_k}, \tag{2.1}$$

where coefficients $a_1, a_2, \ldots, a_m$ are determined by solving the linear system

$$\sum_{k=1}^{m} a_k \frac{\sin \Omega(t_n - t_k)}{t_n - t_k} = f(t_n), \quad n = 1, 2, \ldots, m. \tag{2.2}$$

It was proved in [6] that the MMSE estimator $\Phi_m(t)$ is identical to the minimum energy band-limited interpolant. It was also shown in [21] that the MMSE estimator $\Phi_m(t)$ is the pointwise minimum-error estimator in the worst case.

Furthermore, we have the following error estimate for the MMSE estimator $\Phi_m(t)$ (see [18, Eq. (13)]:

$$|f(t) - \Phi_m(t)| < O\sqrt{E(f)}\frac{\Omega^{1/2}}{m(m\sigma)^m} \quad \forall t \in [-\tau, \tau], \tag{2.3}$$

where $O = e^{-1/2}(2\pi)^{1/2}$, $\sigma = 1/(2e\tau\Omega)$ and $E(f)$ is the energy of f. Thus, given the number m of samples and the bandwidth Ω of $f(t)$, we can determine the condition on τ so that the error bound is small in the interval $[-\tau, \tau]$. It is clear from (2.3) that we need

$$m\sigma > 1, \quad \text{or} \quad \tau < \frac{m}{2e\Omega},$$

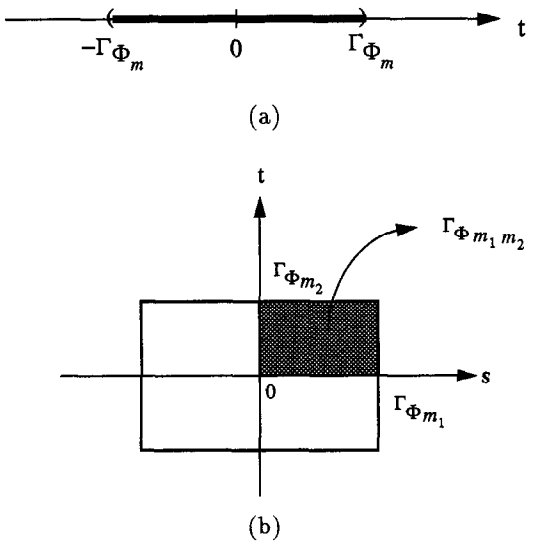

Fig. 2. Critical points in (a) 1-D and (b) 2-D cases.

and a larger $m\sigma$ (or a smaller τ) implies a smaller error bound. Also, increasing the number m of samples tightens the error bound. These motivate the following definitions. The ratio

$$\Gamma_{\Phi_m} \triangleq \frac{m}{2e\Omega} \tag{2.4}$$

is called the *critical value* for the interpolant $\Phi_m(t)$ and the interval $[-\Gamma_{\Phi_m}, \Gamma_{\Phi_m}]$ is called the *critical region*. We conclude that the $\Phi_m(t)$ is a good approximation of $f(t)$ if $|t|$ belongs to the critical region as shown in Fig. 2(a). Different interpolants may have different critical regions, and we can use the critical value as one performance measure. In this paper, when we say that an interpolant $\Psi_1(t)$ is better than another one $\Psi_2(t)$, it is meant that

$$\Gamma_{\Psi_1} \geqslant \Gamma_{\Psi_2}.$$

That is, $\Phi_1(t)$ can approximate $f(t)$ relatively well in a larger interval.

The MMSE estimator can also be extended to the 2-D case (see [6] for more details). Let $f(s, t)$ be (Ω_1, Ω_2) band-limited, i.e., $\hat{f}(\omega_1, \omega_2) = 0$ when $|\omega_1| > \Omega_1$ or $|\omega_2| > \Omega_2$, so that

$$\hat{f}(\omega_1, \omega_2) = \int_{-\infty}^{\infty}\int_{-\infty}^{\infty} f(s, t)e^{-j(s\omega_1 + t\omega_2)}\,ds\,dt,$$

$$f(s, t) = \int_{-\Omega_2}^{\Omega_2}\int_{-\Omega_1}^{\Omega_1} f(\omega_1, \omega_2)e^{j(s\omega_1 + t\omega_2)}\,d\omega_1 d\omega_2.$$

Let $f(s_{i_1}, t_{i_2})$, $i_1 = 1, 2, \ldots, m_1$, $i_2 = 1, 2, \ldots, m_2$, be given samples of $f(s, t)$. Then, the MMSE estimator of $f(s, t)$ from these samples is

$$\Phi_{m_1 m_2}(s, t) = \sum_{i_1=1}^{m_1}\sum_{i_2=1}^{m_2} a_{i_1 i_2}\frac{\sin\Omega_1(s - s_{i_1})}{s - s_{i_1}} \times\frac{\sin\Omega_2(t - t_{i_2})}{t - t_{i_2}}, \tag{2.5}$$

where coefficients $a_{i_1 i_2}$ satisfy

$$\sum_{i_1=1}^{m_1}\sum_{i_2=1}^{m_2} a_{i_1 i_2}\frac{\sin\Omega_1(s_{n_1} - s_{i_1})}{s_{n_1} - s_{i_2}}\frac{\sin\Omega_2(t_{n_2} - t_{i_2})}{t_{n_2} - t_{i_2}} = f(s_{n_1}, t_{n_2}) \tag{2.6}$$

for $n_1 = 1, 2, \ldots, m_1$ and $n_2 = 1, 2, \ldots, m_2$. For the error estimation, Xia et al. [36] extended the error bound (2.3) and obtained the following results.

Proposition 1. *Let $f(s, t)$ be (Ω_1, Ω_2) band-limited. If $f(s, t) \in L^1(R^2)$, i.e.*

$$\int_{R^2} |f(s, t)|\,ds\,dt < \infty,$$

then

$$|f(s, t) - \Phi_{m_1 m_2}(s, t)| < O_1\left(\frac{1}{m_1(m_1\sigma_1)^{m_1}} + \frac{1}{m_2(m_2\sigma_2)^{m_2}}\right), \quad \forall |s| \leqslant \tau_1, |t| \leqslant \tau_2, \tag{2.7}$$

where

$$O_1 = \frac{8\sqrt{2}}{\pi^3}e^{\pi - 1/6}\Omega_1\Omega_2\int_{R^2}|f(s, t)|\,ds\,dt,$$

and $\sigma_l = \dfrac{1}{2e\tau_l\Omega_l}$, $l = 1, 2$

and $|s_{i_1}| \leqslant \tau_1$ and $|t_{i_2}| \leqslant \tau_2$ for all possible i_1 and i_2 with arbitrarily given values of τ_1 and τ_2.

Proposition 2. *Let $f(s, t)$ be (Ω_1, Ω_2) band-limited. If its Fourier spectrum $\hat{f}(\omega_1, \omega_2)$ is second-order differentiable, then*

$$|f(s,t) - \Phi_{m_1m_2}(s,t)| < O_2\left(\frac{1}{m_1(m_1\sigma_1)^{m_1}} + \frac{1}{m_2(m_2\sigma_2)^{m_2}}\right), \quad \forall |s| \leqslant \tau_1, |t| \leqslant \tau_2, \tag{2.8}$$

where

$$O_2 = \frac{2\sqrt{2}}{\pi^3} e^{-1/12}\Omega_1\Omega_2 \sum_{n_1,n_2} |b_{n_1n_2}| < \infty$$

and

$$\sigma_l = \frac{1}{2e\tau_l\Omega_l}, \quad l = 1,2 \tag{2.9}$$

and $|s_{i_1}| \leqslant \tau_1$ and $|t_{i_2}| \leqslant \tau_2$ for all possible i_1 and i_2 with arbitrarily given values of τ_1 and τ_2. The values $b_{n_1n_2}$ in (2.8) are Fourier coefficients of $\hat{f}(\omega_1, \omega_2)$ in $[-\Omega_1, \Omega_1]\times[-\Omega_2, \Omega_2]$.

Although the constants O_1 and O_2 are different in error bounds (2.7) and (2.8), they have the same main term. Similar to the 1-D case, we can also determine the critical region for the interpolant $\Phi_{m_1m_2}$. To have $m_l\sigma_l > 1$, $l = 1,2$, we require

$$\tau_l < \frac{m_l}{2e\Omega_l} = \Gamma_{\Phi_{m_l}}, \quad l = 1,2,$$

which is the critical region of $\Phi_{m_1m_2}$. We plot the critical region in Fig. 2(b) as a square enclosed by the solid line, in which $\Phi_{m_1m_2}(s, t)$ provides a good approximation for $f(s, t)$. Furthermore, we choose

$$\Gamma_{\Phi_{m_1m_2}} \triangleq \frac{m_1m_2}{4e^2\Omega_1\Omega_2} = \Gamma_{\Phi_{m_1}}\Gamma_{\Phi_{m_2}} \tag{2.10}$$

to be the critical value corresponding to the area of a quarter of the critical region (i.e. the dark region in Fig. 2(b)). Thus, we can also measure the performance of a 2-D interpolant with its critical value.

3. 1-D multiband signal reconstruction

3.1. General multiband signals

We consider the reconstruction of a 1-D multiband signal $f(t)$ with its Fourier spectrum shown in Fig. 1, where $B_k > 0$ and C_k with $|k| \leqslant K$, are known a priori and $C_k - C_{k-1} \geqslant B_k + B_{k-1}$. The $f(t)$ can be represented as

$$f(t) = \sum_{k=-K}^{k} f_k(t)e^{-jtC_k}, \tag{3.1}$$

where $f_k(t)$ is B_k band-limited. Since the bandwidth Ω of $f(t)$ is often much larger than each B_k of $f_k(t)$, the critical value of the MMSE estimator for $f(t)$ is much smaller than that for $f_k(t)$. This observation motivates us to use the MMSE estimator of $f_k(t)$ with $|k| \leqslant K$ for the reconstruction of $f(t)$.

Let $S \triangleq \{t_1, t_2, \ldots, t_m\} \subset [-T, T]$ for certain $T > 0$ be the set of selected sampling points, and $S_k \triangleq \{t_{k1}, t_{k2}, \ldots, t_{km_k}\} \subset [-T, T]$ be the set of arbitrarily fixed m_k distinct points, where m_k satisfies

$$\sum_{k=-K}^{K} m_k = m.$$

Then, a new reconstruction interpolant can be obtained via

$$\Psi_m(t) = \sum_{k=-K}^{K}\sum_{i=1}^{m_k} a_{ki}\frac{\sin B_k(t - t_{ki})}{t - t_{ki}} e^{-jtC_k}, \tag{3.2}$$

where coefficients a_{ki} satisfy the following system:

$$\sum_{k=-K}^{K}\sum_{i=1}^{m_k} a_{ki}\frac{\sin B_k(t_n - t_{ki})}{t_n - t_{ki}} e^{-jt_nC_k} = f(t_n), \quad n = 1,2,\ldots,m. \tag{3.3}$$

Note that the points t_{ki} in S_k are arbitrarily chosen in $[-T, T]$ and may not be related to the sampling points in S.

Remark. When the parameters in (3.2)–(3.3) are the following: $m_0 = m$, $m_k = 0$ for $k \neq 0$, $a_{0,i} = a_i$ and $t_{0,i} = t_i$, then the interpolant $\Psi_m(t)$ in (3.2) is the band-passed version of the MMSE estimator $\Phi_m(t)$ in (2.1) where the band-pass filter has the pass regions the same as the ones in Fig. 1.

It is clear from (2.4) that, to keep the critical value constant, the larger the bandwidth B_k of the kth signal $f_k(t)$ the more points m_k we need in S_k, so that

$$\sum_{i=1}^{m_k} a_{ki}\frac{\sin B_k(t - t_{ki})}{t - t_{ki}}$$

approximates $f_k(t)$ well. Thus, we impose the following constraint on the size m_k of the set S_k:

$$\frac{m_k}{B_k} = r, \quad k = -K, -K+1, \ldots, K, \tag{3.4}$$

where r is a positive constant. With (3.4) we have

$$r = \frac{\sum_{k=-K}^{K} m_k}{\sum_{k=-K}^{K} B_k} = \frac{m}{\sum_{k=-K}^{K} B_k}. \tag{3.5}$$

The following theorem gives an error bound for the reconstruction interpolant $\Psi_m(t)$ given by (3.2).

Theorem 1. *Let $f(t)$ be a multiband signal with parameters as stated before. If the coefficient matrix for unknowns a_{ki} in (3.3) is of full rank, then*

$$|f(t) - \Psi_m(t)| < Or \sum_{k=-K}^{K} \left(\frac{2e\tau}{r}\right)^{m_k}$$

$$\text{for } t \in [-\tau, \tau], \tag{3.6}$$

where $\tau \geqslant T$, r is defined in (3.5) and O is a positive constant.

The proof of Theorem 1 is given in Appendix A. The coefficient matrix in (3.3) often has a full rank. If not, one can adjust the points in S_k to make it a full rank matrix. Details depend on the sampling points t_n and the subband bandwidths Ω_n.

Based on the error bound (3.6), the critical value Γ_{Ψ_m} for the interpolant $\Psi_m(t)$ can be defined as

$$\Gamma_{\Psi_m} = \frac{r}{2e} = \frac{m}{2e\sum_{k=-K}^{K} B_k} = \frac{\Omega}{\sum_{k=-K}^{K} B_k} \Gamma_{\Phi_m}. \tag{3.7}$$

We see that the critical value Γ_{Ψ_m} is reciprocally related to the total size of occupied bands, i.e. $2\sum_{k=-K}^{K} B_k$. Furthermore, since $\sum_{k=-K}^{K} B_k \leqslant \Omega$, we have

$$\Gamma_{\Psi_m} \geqslant \Gamma_{\Phi_m}. \tag{3.8}$$

This means that the length of the critical interval of the interpolant Ψ_m given by (3.2) for an Ω band-limited signal with a multiband structure is always greater than or equal to that of its MMSE estimator Φ_m without exploiting the multiband feature. In addition, when the multiband signal $f(t)$ does not fully occupy the band $[-\Omega, \Omega]$, the critical value Γ_{Ψ_m} of our proposed method is strictly greater than the critical value Γ_{Φ_m} of the MMSE estimator. We call

$$\gamma_1 \triangleq \frac{\Omega}{\sum_{k=-K}^{K} B_k},$$

the *gain factor*. When the band $[-\Omega, \Omega]$ is fully occupied, the gain factor is 1 (no gain).

When all B_k are equal, the error bound in (3.6) can be simplified.

Corollary 1. *Let $f(t)$ be a multiband signal with parameters as before and $B_k = B$ for all k. If the coefficient matrix for unknowns a_{ki} in (3.3) is of full rank, then*

$$|f(t) - \Psi_m(t)| < O(2K+1)r \left(\frac{2er}{r}\right)^{m/(2K+1)}$$

$$\text{for } t \in [-\tau, \tau], \tag{3.9}$$

where

$$r = \frac{m}{(2K+1)B}.$$

3.2. Real multiband signals

As a special case of multiband signals $f(t)$ in (3.1), we assume all $f_k(t)$ and $f(t)$ to be real in this subsection. The signal $f(t)$ can be represented as

$$f(t) = \sum_{k=0}^{K} f_k(t)\cos(C_k t), \tag{3.10}$$

where $f_k(t)$ is real B_k band-limited for $k = 0, 1, 2, \ldots, K$. A typical Fourier spectrum for this class of signals is shown in Fig. 3, where $B_{-k} = B_k$.

For $f(t)$ given by (3.10), we can use another interpolant instead of the one in (3.2)–(3.3), i.e.

$$\tilde{\Psi}_m(t) = \sum_{k=0}^{K} \sum_{i=1}^{m_k} a_{ki} \frac{\sin B_k(t - t_{ki})}{t - t_{ki}} \cos(C_k t),$$

where t_{ki} with $i = 1, 2, \ldots, m_k$ are arbitrarily fixed distinct points in $[-T, T]$ for each k,

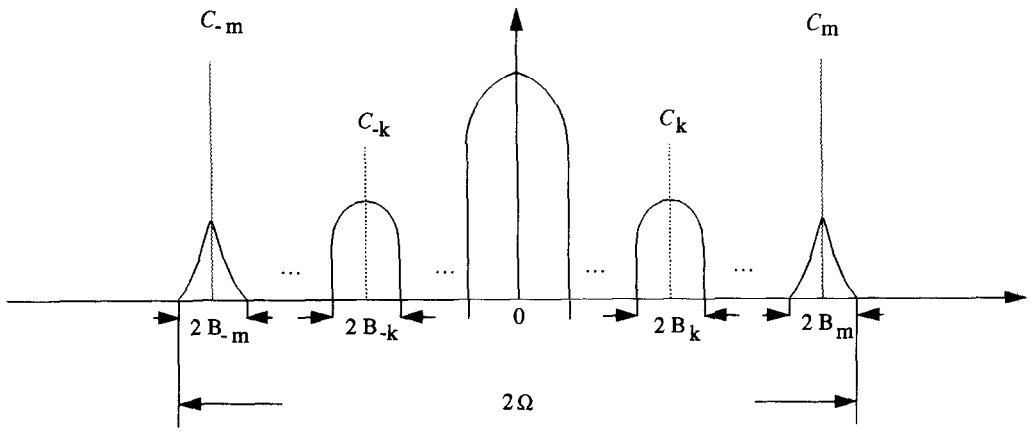

Fig. 3. Fourier spectrum of a modulated real signal.

$\sum_{k=0}^{K} m_k = m$ and a_{ki} are obtained via solving the system

$$\sum_{k=0}^{K}\sum_{i=1}^{m_k} a_{ki}\frac{\sin B_k(t_n - t_{ki})}{t_n - t_{ki}}\cos(C_k t_n) = f(t_n),$$

$$n = 1, 2, \ldots, m.$$

We can derive an error bound for $\tilde{\Psi}_m(t)$ similar to that given in Theorem 1 as

$$|f(t) - \tilde{\Psi}_m(t)| < O\tilde{r}\sum_{k=0}^{K}\left(\frac{2e\tau}{\tilde{r}}\right)^{m_k}, \quad t \in [-\tau, \tau],$$

where O is as before and

$$\tilde{r} = \frac{m}{\sum_{k=0}^{K} B_k}.$$

In particular, if $B_k = B$ for $k = 0, 1, 2, \ldots, K$, we have a result similar to Corollary 1, i.e.

$$|f(t) - \tilde{\Psi}_m(t)| < O\tilde{r}\left(\frac{2e\tau}{\tilde{r}}\right)^{m/(K+1)}, \quad t \in [-\tau, \tau].$$

The critical value for this case is

$$\Gamma_{\tilde{\Psi}_m} = \frac{m}{2e\sum_{k=0}^{K} B_k} = \frac{\sum_{k=-K}^{K} B_k}{\sum_{k=0}^{K} B_k}\Gamma_{\Psi_m} = \left(1 + \frac{\sum_{k=1}^{K} B_k}{\sum_{k=0}^{K} B_k}\right)\Gamma_{\Psi_m}, \tag{3.11}$$

Combining (3.8) and (3.11), we obtain

$$\Gamma_{\tilde{\Psi}_m} > \Gamma_{\Psi_m} \geqslant \Gamma_{\Phi_m} \quad \text{for } K > 0.$$

Besides, it is straightforward to derive that

$$\Gamma_{\tilde{\Psi}_m} = \gamma_2 \Gamma_{\Phi_m},$$

where

$$\gamma_2 \triangleq \frac{\Omega}{\sum_{k=0}^{K} B_k}$$

is the gain factor for $\tilde{\Psi}_m$ with the MMSE estimate Φ_m as the reference. It is interesting to point out that γ_2 is always greater than 1 if $K > 0$. When the bandwidth B_0 of the base band is small with

$$\frac{\sum_{k=1}^{K} B_k}{\sum_{k=0}^{K} B_k} \approx 1,$$

we can simplify (3.11) to be

$$\Gamma_{\tilde{\Psi}_m} \approx 2\Gamma_{\Psi_m} \geqslant 2\Gamma_{\Phi_m},$$

so that the gain factor $\gamma_2 \geqslant 2$. This implies that the interpolant $\tilde{\Psi}_m$ for modulated real signals performs almost at least twice as well as the MMSE estimator Γ_{Φ_m}. This point will be demonstrated in numerical examples in Section 5.

4. 2-D multiband signal reconstruction

4.1. General multiband signals

Now, let us consider 2-D multiband signals $f(s, t)$ with $2K + 1$ nonoverlaping multibands

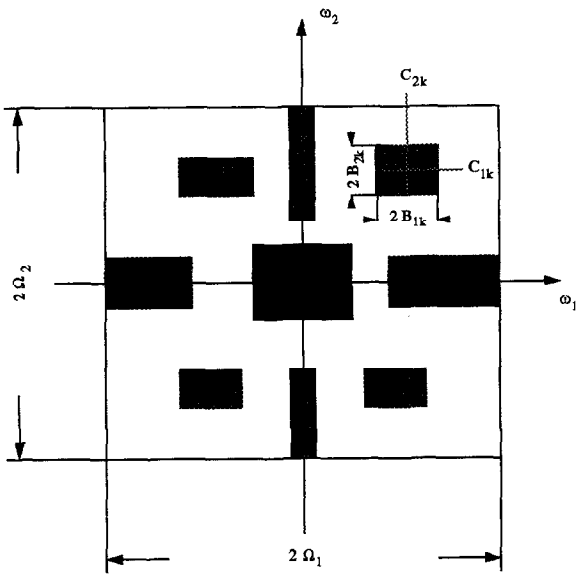

Fig. 4. Occupied bands in the frequency domain of 2-D multiband signals.

bounded by $[-\Omega_1, \Omega_1]\times[-\Omega_2, \Omega_2]$ as shown in Fig. 4, where each band, with index $-K \leqslant k \leqslant K$ has the center frequencies C_{1k} and C_{2k} and bandwidths B_{1k} and B_{2k} along the frequency axes ω_1 and ω_1, respectively. We assume that these multiband parameters are known a priori. It is clear that

$$\sum_{k=-K}^{K} B_{1k}B_{2k} \leqslant \Omega_1\Omega_2. \tag{4.1}$$

The 2-D multiband signal $f(s, t)$ can be represented by

$$f(s,t) = \sum_{k=-K}^{K} f_k(s,t)\mathrm{e}^{-\mathrm{j}(sC_{1k}+tC_{2k})}, \tag{4.2}$$

where $f_k(s, t)$ is (B_{1k}, B_{2k}) band-limited while $f(s, t)$ is (Ω_1, Ω_2) band-limited. The reconstruction problem is to recover $f(s, t)$ from its samples $f(s_{i_1}, t_{i_2})$, $i_l = 1, 2, \ldots, m_l$, $l = 1, 2$, where the sampling points are selected from $[-T_1, T_1]\times[-T_2, T_2]$ for some $T_1, T_2 > 0$.

Let

$$S_k = \{(s_{ki_1}, t_{ki_2}) \in [-T_1, T_1]\times[-T_2, T_2]:$$
$$i_l = 1, 2, \ldots, m_{lk},\ l = 1, 2\},\quad |k| \leqslant K$$

be a set of arbitrarily fixed $m_{1k}m_{2k}$ distinct points, where

$$\sum_{k=-K}^{K} m_{1k}m_{2k} = m_1m_2. \tag{4.3}$$

Similar to the interpolant $\Psi_m(t)$ in the 1-D case, we have the following $\Psi_{m_1m_2}(s, t)$ for the reconstruction of $f(s, t)$:

$$\Psi_{m_1m_2}(s,t) = \sum_{k=-K}^{K}\sum_{i_1=1}^{m_{1k}}\sum_{i_2=1}^{m_{2k}} a_{ki_1i_2}\frac{\sin B_{1k}(s-s_{ki_1})}{s-s_{ki_1}} \times\frac{\sin B_{2k}(t-t_{ki_2})}{t-t_{ki_2}}\mathrm{e}^{-\mathrm{j}(sC_{1k}+tC_{2k})}, \tag{4.4}$$

where $a_{ki_1i_2}$ satisfy the following system:

$$\sum_{k=-K}^{K}\sum_{i_1=1}^{m_{1k}}\sum_{i_2=1}^{m_{2k}} a_{ki_1i_2}\frac{\sin B_{1k}(s_{n_1}-s_{ki_1})}{s_{n_1}-s_{ki_1}} \times\frac{\sin B_{2k}(t_{n_2}-t_{ki_2})}{t_{n_2}-t_{ki_2}}\mathrm{e}^{-\mathrm{j}(s_{n_1}C_{1k}+t_{n_2}C_{2k})} = f(s_{n_1}, t_{n_2}) \tag{4.5}$$

for $n_l = 1, 2, \ldots, m_l$ and $l = 1, 2$.

We next estimate the error bound and analyze the critical region of $\Psi_{m_1m_2}(s, t)$. Similar to the assumption (3.4) in the 1-D case, we assume that

$$\frac{m_{lk}}{B_{lk}} = r_l,\quad l = 1, 2,\quad \text{and}$$
$$k = -K, -K+1, \ldots, K, \tag{4.6}$$

where r_1 and r_2 are constants. Thus, by (4.3), we have

$$r_1r_2\sum_{k=-K}^{K} B_{1k}B_{2k} = \sum_{k=-K}^{K} m_{1k}m_{2k} = m_1m_2$$

and, therefore,

$$r_1r_2 = \frac{m_1m_2}{\sum_{k=-K}^{K} B_{1k}B_{2k}}. \tag{4.7}$$

Then, we have the following theorem on the error bound of $\Psi_{m_1m_2}(t)$.

Theorem 2. *Consider a function $f(s, t)$ of the form (4.2). For all $k = -K, -K+1, \ldots, K$, if*
(i) $f_k(s, t) \in L^1(\boldsymbol{R})$, *or*

(ii) $\hat{f}(\omega_1, \omega_2)$ *is second-order differentiable in* $[-B_{1k}, B_{1k}] \times [-B_{2k}, B_{2k}]$,

and the coefficient matrix for unknowns $a_{ki_1i_2}$ *in* (4.5) *is of full rank, then*

$$|f(s,t) - \Psi_{m_1m_2}(s,t)| \leqslant O \sum_{k=-K}^{K} \left(\left(\frac{2e\tau_1}{r_1} \right)^{m_{1k}} + \left(\frac{2e\tau_2}{r_2} \right)^{m_{2k}} \right)$$

$$\text{for } |s| \leqslant \tau_1, |t| \leqslant \tau_2, \tag{4.8}$$

where $\tau_l \geqslant T_l$ *for* $l = 1, 2$, O *is a positive constant and* r_1, r_2 *are as in* (4.6).

Since the proof of Theorem 2 is similar to that of Theorem 1, it is omitted. In the uniform multiband case, the estimate in (4.8) can be simplified further.

Corollary 2. *If the same conditions stated in Theorem 2 are satisfied and if* $B_{lk} = B_l$, *for* $|k| \leqslant K$ *and* $l = 1, 2$, *then*

$$|f(s,t) - \Psi_{m_1m_2}(s,t)| \leqslant O\left(\left(\frac{2e\tau_1}{r_1} \right)^{r_1B_1} + \left(\frac{2e\tau_2}{r_2} \right)^{r_2B_2} \right)$$

$$\text{for } |s| \leqslant \tau_1, |t| \leqslant \tau_2. \tag{4.9}$$

Based on error bounds (4.8) and (4.9), the critical value for $\Psi_{m_1m_2}$ is

$$\Gamma_{\Psi_{m_1m_2}} = r_1r_2/(4e^2).$$

By using (2.10) and (4.7), we can relate this critical value to that of the MMSE estimator $\Phi_{m_1m_2}$ in (2.5) as

$$\Gamma_{\Psi_{m_1m_2}} = \frac{m_1m_2}{4e^2 \sum_{k=-K}^{K} B_{1k}B_{2k}} = \frac{\Omega_1\Omega_2}{\sum_{k=-K}^{K} B_{1k}B_{2k}} \Gamma_{\Phi_{m_1m_2}},$$

so that the gain factor is

$$\gamma_3 \triangleq \frac{\Omega_1\Omega_2}{\sum_{k=-K}^{K} B_{1k}B_{2k}}.$$

It is clear from (4.1) that $\gamma_3 \geqslant 1$. Moreover, if the band $[-\Omega_1, \Omega_1] \times [-\Omega_2, \Omega_2]$ is not fully occupied, the gain factor $\gamma_3 > 1$. Thus, we conclude the new algorithm is better than the MMSE estimator for (Ω_1, Ω_2) band-limited signals with a multiband structure.

4.2. Real multiband signals

When $f_k(s,t)$ and $f(s,t)$ in (4.2) are real signals, we can find a more efficient reconstruction algorithm. The $f(s,t)$ can be represented as

$$f(s,t) = \sum_{k=0}^{K} f_k(s,t) \cos(sC_{1k} + tC_{2k}).$$

Note that its spectrum $\hat{f}(\omega_1, \omega_2)$ has the symmetry with respect to the origin, i.e.

$$\hat{f}(\omega_1, \omega_2) = \hat{f}(-\omega_1, -\omega_2).$$

For $k = 0, 1, \ldots, K$, we use S_k to denote the set of auxiliary sampling points and

$$\sum_{k=0}^{K} m_{1k}m_{2k} = m_1m_2.$$

Then, we can use the following interpolant as an approximation for the real multiband signal $f(s,t)$:

$$\tilde{\Psi}_{m_1m_2}(s,t) = \sum_{k=0}^{K} \sum_{i_1=1}^{m_{1k}} \sum_{i_2=1}^{m_{2k}} a_{ki_1i_2} \frac{\sin B_{1k}(s - s_{ki_1})}{s - s_{ki_1}} \times \frac{\sin B_{2k}(t - t_{ki_2})}{t - t_{ki_2}} \cos(sC_{1k} + tC_{2k}),$$

where coefficients $a_{ki_1i_2}$ satisfy the following system:

$$\sum_{k=0}^{K} \sum_{i_1=1}^{m_{1k}} \sum_{i_2=1}^{m_{2k}} a_{ki_1i_2} \frac{\sin B_{1k}(s_{n_1} - s_{ki_1})}{s_{n_1} - s_{ki_1}} \times \frac{\sin B_{2k}(t_{n_2} - t_{ki_2})}{t_{n_2} - t_{ki_2}} \cos(s_{n_1}C_{1k} + t_{n_2}C_{2k}) = f(s_{n_1}, t_{n_2})$$

for $n_l = 1, 2, \ldots, m_l$ and $l = 1, 2$. The error bound on the interpolant $\tilde{\Psi}_{m_1m_2}(s,t)$ is

$$|f(s,t) - \tilde{\Psi}_{m_1m_2}(s,t)| \leqslant O \sum_{k=0}^{K} \left(\left(\frac{2e\tau_1}{\tilde{r}_1} \right)^{m_{1k}} + \left(\frac{2e\tau_2}{\tilde{r}_2} \right)^{m_{2k}} \right)$$

$$\text{for } |s| \leqslant \tau_1, |t| \leqslant \tau_2,$$

where $\tau_l \geqslant T_l$ for $l = 1, 2$, O the same as in (4.8) and

$$\tilde{r}_1\tilde{r}_2 = \frac{m_1m_2}{\sum_{k=0}^{K} B_{1k}B_{2k}}. \tag{4.10}$$

By using (2.10), (4.7) and (4.10), we can compute the critical value for this case as

$$\Gamma_{\tilde{\Psi}_{m_1m_2}} = \frac{\tilde{r}_1\tilde{r}_2}{4e^2} = \frac{\tilde{r}_1\tilde{r}_2}{r_1r_2}\frac{r_1r_2}{4e^2} = \frac{\sum_{k=-K}^{K} B_{1k}B_{2k}}{\sum_{k=0}^{K} B_{1k}B_{2k}}\Gamma_{\Psi_{m_1m_2}}$$

$$= \frac{\Omega_1\Omega_2}{\sum_{k=0}^{K} B_{1k}B_{2k}}\Gamma_{\Phi_{m_1m_2}}.$$

Therefore, we have the gain factor

$$\gamma_4 = \frac{\Omega_1\Omega_2}{\sum_{k=0}^{K} B_{1k}B_{2k}}.$$

If the bandwidth B_0 of the base band is small, we have

$$\frac{\sum_{k=-K}^{K} B_{1k}B_{2k}}{\sum_{k=0}^{K} B_{1k}B_{2k}} \approx 2.$$

Consequently, $\Gamma_{\tilde{\Psi}_{m_1m_2}} \approx 2\Gamma_{\Psi_{m_1m_2}} \geqslant 2\Gamma_{\Phi_{m_1m_2}}$ and $\gamma_4 \geqslant 2$. Note also that if the signal has symmetric spectrum with respect to both ω_1 and ω_2 axes, it can be expressed as

$$f(s,t) = \sum_{k=0}^{K} f_k(s,t)\cos(sC_{1k})\cos(tC_{2k}).$$

It is possible to modify the above algorithm so that it achieves a gain factor $\gamma_5 \geqslant 4$.

5. Numerical experiments

We use numerical examples to demonstrate the performance of the proposed algorithms.

Test problem 1: 1-D multiband signal. The test signal is chosen to be the modulated real signals

$$f(t) = f_0(t) + 0.5f_1(t)\cos(C_1t),$$

with the Fourier spectrum

$$\hat{f}_k(\omega) = \begin{cases} \pi\sin(\alpha_k|\omega|), & |\omega| \leqslant B_k, \\ 0, & |\omega| > B_k, \end{cases}$$

where $k = -1, 0, 1$, and α_k and B_k are positive constants. Since $f(t)$ is real, $\hat{f}_k(-\omega) = \hat{f}_k^*(\omega)$. In the experiment, we choose

$$\alpha_0 = 4\pi, \quad \alpha_1 = 6\pi,$$

and

$$\Omega = 4\pi, \quad B_0 = \frac{\pi}{8}, \qquad C_1 = \Omega - B_1,$$

where B_1 be a parameter ranging from 0 to $31\pi/16$. Note that, when $B_1 = 31\pi/16$, $B_0 + 2B_1 = \Omega$ so that the band $[-\Omega, \Omega]$ is fully occupied. We observe the function $f(t)$ at uniformly sampled points $t = n/10$ with $n = -10, -9, \ldots, 9$ so that the total number of sampling points is 20. The auxiliary sampling point sets are chosen as subsets of S with $S_1 \cup S_2 = S$.

We compute $\tilde{\Psi}_m$ for the reconstruction of $f(t)$. The critical value for this case is

$$\Gamma_{\tilde{\Psi}_{20}} = \frac{20}{2e(B_0 + B_1)} = \frac{10}{e(\pi/8 + B_1)},$$

which is a function of B_1. The curve of $\Gamma_{\tilde{\Psi}_{20}}$ via B_1 is shown in Fig. 5. The critical point for the MMSE estimator is

$$\Gamma_{\Phi_{20}} = \frac{20}{2e(4\pi)} = \frac{5}{2e\pi},$$

which corresponds to the constant line as shown in Fig. 5. We can clearly see the improvement of our proposed algorithm when the bandwidth B_1 becomes smaller and the band $[-\Omega, \Omega]$ is less fully utilized.

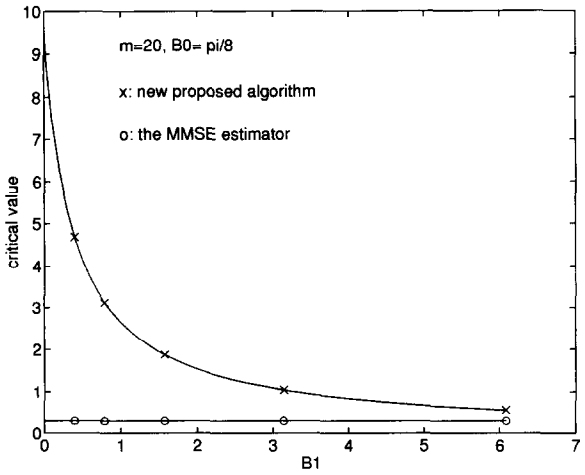

Fig. 5. The critical value curves via B_1 for the algorithm $\tilde{\Psi}_{20}$ and the MMSE estimator Φ_{20}.

To give a more clear performance comparison of various methods, we applied the MMSE estimator $\Phi_{20}(t)$ and the interpolant $\tilde{\Psi}_{20}(t)$ to two test signals with $B_1 = \pi/8$ and $B_1 = 31\pi/16$ and plotted the results in Figs. 6–9. In all these figures, we show the true signal $f(t)$ in (a), its Fourier spectrum $\hat{f}(\omega)$ in (b), the reconstructed function ($\tilde{\Psi}_{20}(t)$ or $\Phi_{20}(t)$) in (c) and the corresponding error ($|\tilde{\Psi}_{20}(t) - f(t)|$ or $|\Phi_{20}(t) - f(t)|$) in (d). In subplot (d), we also indicate the critical region by labelling two boundary points as 'critical point'. When $B_1 = \pi/8$, the signal $f(t)$ consists of three narrow bands. When $B_1 = 31\pi/16$, the signal $f(t)$ is in fact a full-band signal. By comparing the results in Figs. 6 and 7 and those in Figs. 8 and 9, we can clearly see that the proposed method with $\tilde{\Psi}_{20}(t)$ performs much better than the MMSE estimator $\tilde{\Phi}_{20}(t)$ in both cases. Besides, the proposed algorithm performs better when the bandwidth is not fully occupied.

Test problem 2: 2-D multiband signal. The 2-D test is a $(4\pi, 4\pi)$ band-limited real signal of the form

$$f(s,t) = f_0(s,t) + 0.25 f_1(s,t)\cos(C_{11}s + C_{12}t),$$

where $f_k(s,t)$ are (B_{1k}, B_{2k}) band-limited with $B_{1k} = B_{2k} = \pi/4$ for $k = 0, 1$, $C_{11} = C_{12} = 4\pi - \pi/4 = 15\pi/4$. The contour plot of the Fourier spectrum $\hat{f}(\omega_1, \omega_2)$ is given in Fig. 10(a) and the original signal $f(s,t)$ is shown in Fig. 10(b). We choose $m_1 = m_2 = 20$, $m_{10} = m_{11} = 10$ and $m_{20} = m_{21} = 20$. The sampling point set is $S = \{(n_1/10, n_2/10)$: for $n_i = -10, -9, \ldots, 9$ for $i = 1, 2\}$, which is concentrated in $[-1, 1] \times [-1, 1]$. The auxiliary sampling point sets S_0 and S_1 are also chosen as subsets of S. The reconstruction $\Phi_{20,20}(s,t)$ from the MMSE estimator and the reconstruction $\tilde{\Psi}_{20,20}(s,t)$ from our proposed method are shown in Figs. 11(a) and (b), respectively. We can clearly see that the new method gives a more accurate result over a larger domain. We also show the absolute error of these two methods in Figs. 12 and 13 with both surface and contour plots. The improvement is clear from these plots.

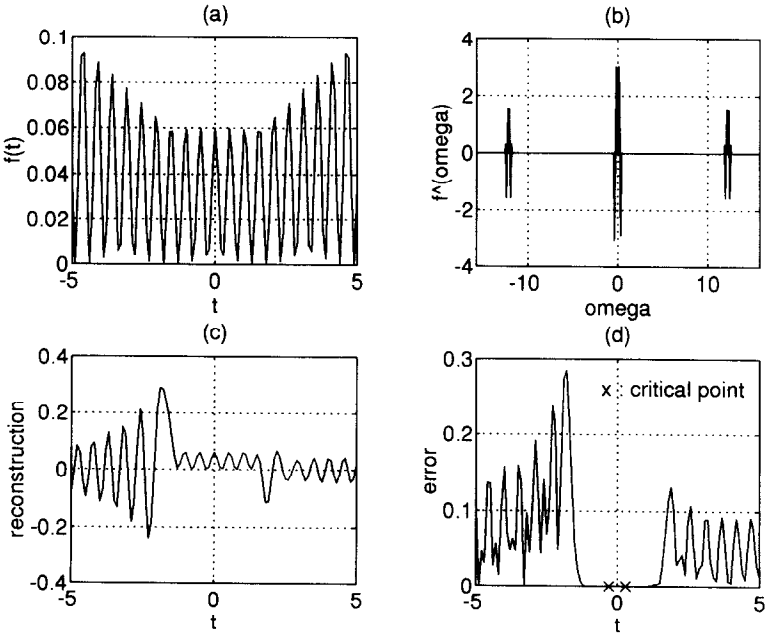

Fig. 6. Results with $\Phi_{20}(t)$ for $B_1 = \pi/8$.

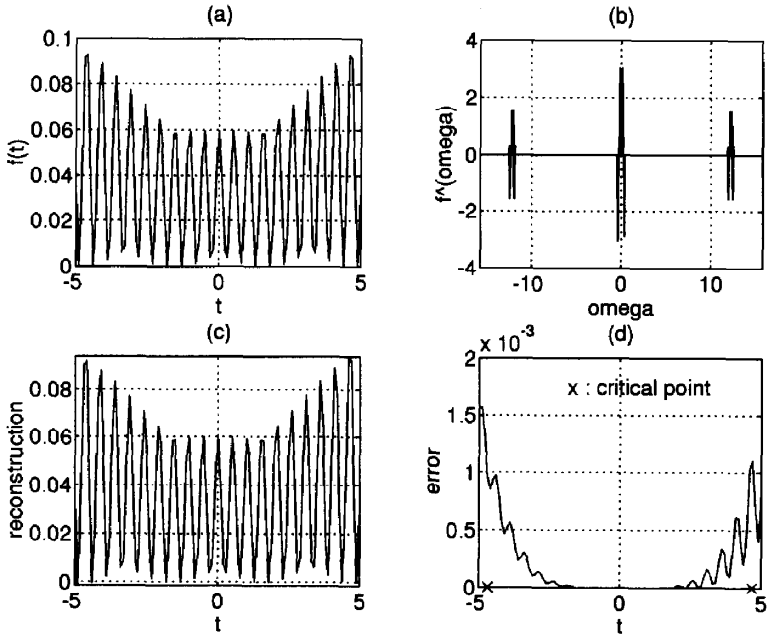

Fig. 7. Results with $\tilde{\Psi}_{20}(t)$ for $B_1 = \pi/8$.

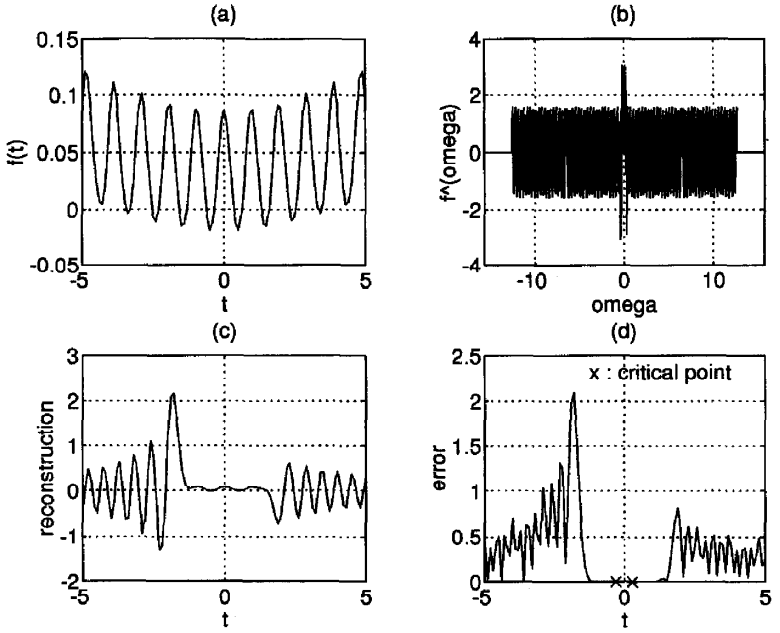

Fig. 8. Results with $\Phi_{20}(t)$ for $B_1 = 31\pi/16$.

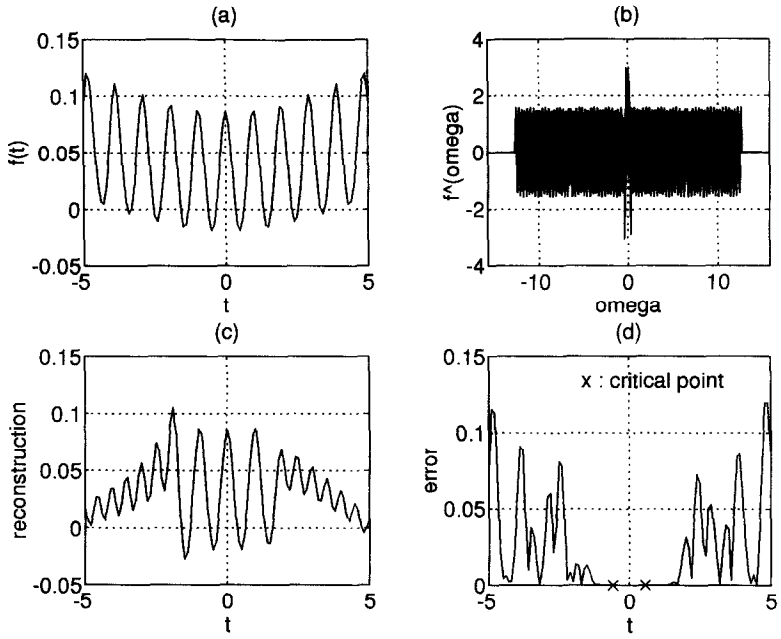

Fig. 9. Results with $\tilde{\Psi}_{20}(t)$ for $B_1 = 31\pi/16$.

6. Conclusions

We proposed a new reconstruction algorithm for a band-limited signal with a multiband structure from its finite samples. The concept of critical regions and values for a reconstruction algorithm was introduced for the performance measure. Based on this criterion, we can clearly see the improvement of our new algorithm for band-limited/multiband signals over the MMSE estimator for general band-limited signals. We also gave numerical experiments to support the theoretical derivation.

Acknowledgements

The authors wish to thank the anonymous reviewers for their encouragement and detailed comments which improve the clarity of this manuscript.

Appendix A. Proof of Theorem 1

Let $\boldsymbol{a}$ denote the solution vector for the system (3.3), and A be the coefficient matrix. Let $\boldsymbol{f}$ be the constant vector with components $f(t_n)$ in (3.3). Then, we can write (3.3) as

$$A\boldsymbol{a} = \boldsymbol{f}. \tag{A.1}$$

Let $\boldsymbol{a}^{(\alpha)}$ be the Tikhonov regularization solution of the system (A.1) with parameter α, i.e.,

$$\boldsymbol{a}^{(\alpha)} = \frac{A^*\boldsymbol{f}}{A^*A + \alpha I}, \tag{A.2}$$

where A^* is the complex conjugate of the matrix A and I is the $m \times m$ identity matrix. Then, see [27, 29],

$$\|\boldsymbol{a} - \boldsymbol{a}^{(\alpha)}\| \leqslant O_1\sqrt{\alpha}, \tag{A.3}$$

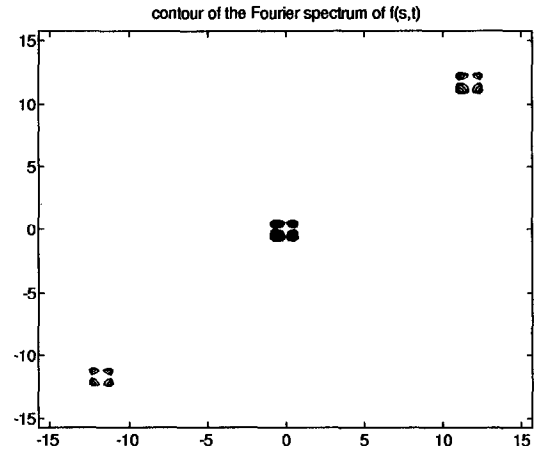

(a)

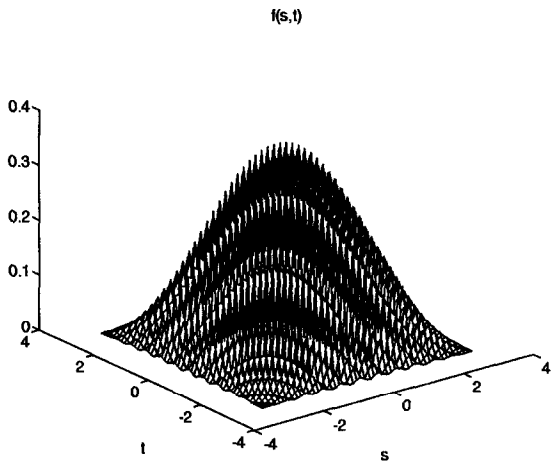

(b)

Fig. 10. (a) The contour plot of $\hat{f}(\omega_1, \omega_2)$ and (b) the surface plot of the exact $f(s, t)$.

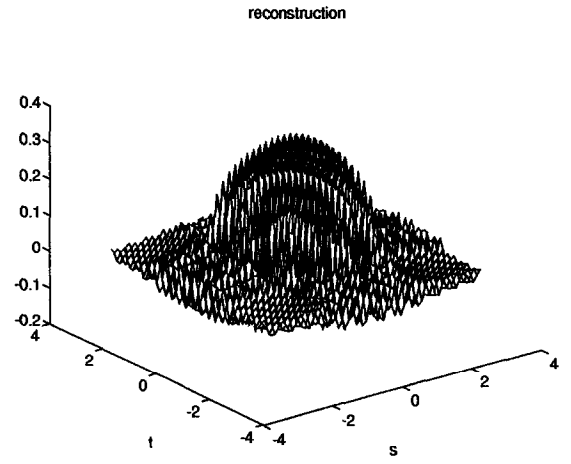

(a)

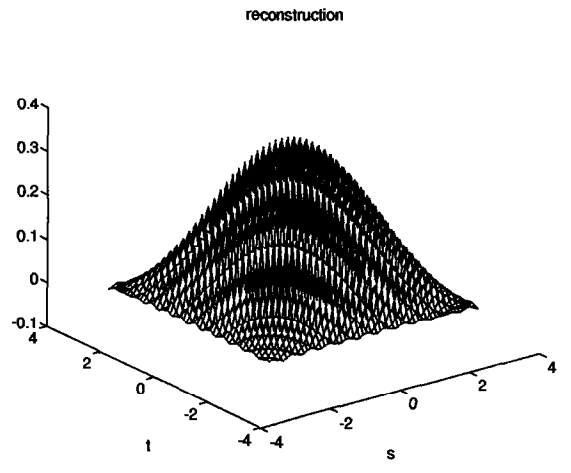

(b)

Fig. 11. The reconstructions: (a) $\Phi_{20,20}(s, t)$ and (b) $\tilde{\Psi}_{20,20}(s, t)$.

where O_1 is a constant which only depends on the signal f. For each k with $-K \leqslant k \leqslant K$, let b_{ki} satisfy the following system:

$$\sum_{i=1}^{m_k} b_{ki} \frac{\sin B_k(t_{kl} - t_{ki})}{t_{kl} - t_{ki}} = f_k(t_{kl})$$

$$\text{for } l = 1, 2, \ldots, m_k. \tag{A.4}$$

Let $\boldsymbol{b}$ denote the vector with components b_{ki} for all possible k, i. From $\boldsymbol{b}$ we have the MMSE estimator

$$\Phi_{m_k}(t) = \sum_{i=1}^{m_k} b_{ki} \frac{\sin B_k(t - t_{ki})}{t - t_{ki}}.$$

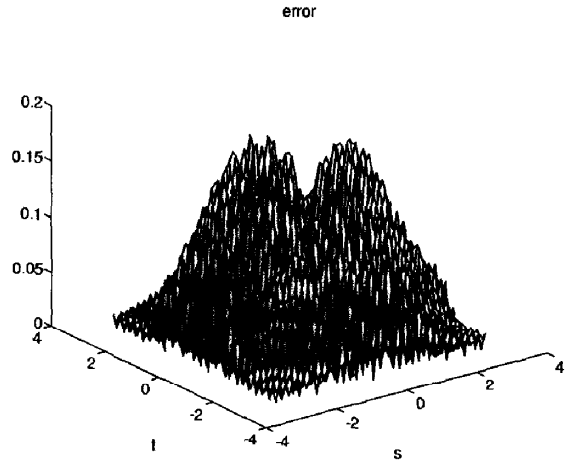

(a)

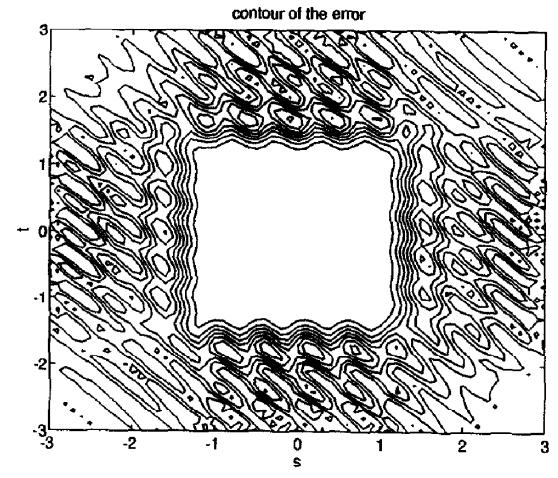

(b)

Fig. 12. The error $\mathrm{err}_2 = |\Phi_{20,20}(s,t) - f(s,t)|$: (a) the surface plot and (b) the contour plot.

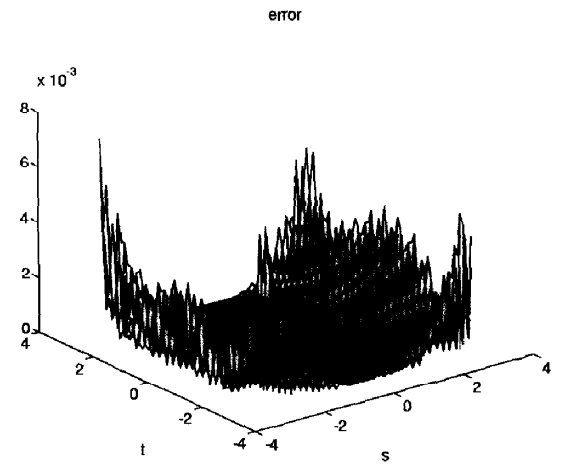

(a)

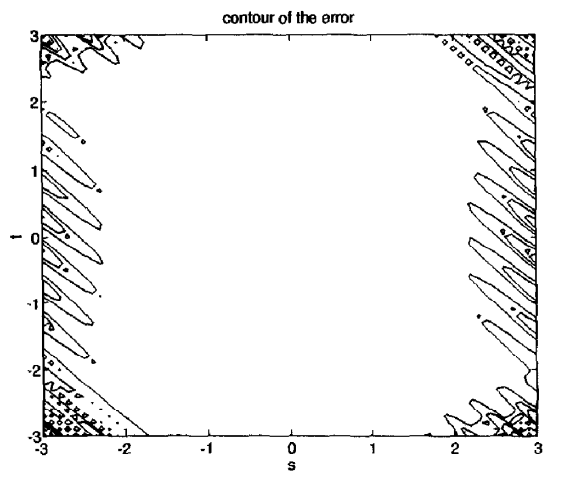

(b)

Fig. 13. The error $\mathrm{err}_1 = |\Psi_{20,20}(s,t) - f(s,t)|$: (a) the surface plot and (b) the contour plot.

Then, by applying the error estimate (2.3) to the kth B_k band-limited signal $f_k(t)$ of $f(t)$,

$$|f_k(t) - \Phi_{m_k}(t)| < O\sqrt{E(f_k)r}\left(\frac{2e\tau}{r}\right)^{m_k}$$

for $t \in [-\tau, \tau]$, (A.5)

where $\tau \geqslant T$ and r is defined in (3.4). Since $t_n \in [-T, T]$, we have

$$|f_k(t_n) - \Phi_{m_k}(t_n)| < O\sqrt{E(f_k)r}\left(\frac{2eT}{r}\right)^{m_k}$$

for $n = 1, 2, \ldots, m$.

Therefore,

$$|(Ab)(n) - f(t_n)| = \left| \sum_{k=-K}^{K} \Phi_{m_k}(t_n) e^{-jt_n C_k} - f(t_n) \right|$$
$$\leqslant \sum_{k=-K}^{K} |\Phi_{m_k}(t_n) - f_k(t_n)|$$
$$\leqslant O\sqrt{E(f)r} \sum_{k=-K}^{K} \left(\frac{2eT}{r}\right)^{m_k}$$
$$\text{for } n = 1, 2, \ldots, m, \tag{A.6}$$

where O is as before. Let

$$b^{(\alpha)} \triangleq \frac{A^*Ab}{A^*A + \alpha I}.$$

Then,

$$\|b - b^{(\alpha)}\| \leqslant O_2\sqrt{\alpha}, \tag{A.7}$$

where O_2 is a positive constant which only depends on the signal f. By (A.1), (A.6) and (A.7),

$$\|a^{(\alpha)} - b^{(\alpha)}\| = \left\| \frac{A^*f}{A^*A + \alpha I} - \frac{A^*Ab}{A^*A + \alpha I} \right\|$$
$$\leqslant \frac{1}{\alpha} \|A^*(Ab - f)\|$$
$$\leqslant O\sqrt{E(f)} \frac{2m}{\alpha} r \sum_{k=-K}^{K} \left(\frac{2eT}{r}\right)^{m_k}.$$

Therefore,

$$\|a - b\| \leqslant \|a - a^{(\alpha)}\| + \|a^{(\alpha)} - b^{(\alpha)}\| + \|b - b^{(\alpha)}\|$$
$$\leqslant (O_1 + O_2)\sqrt{\alpha}$$
$$+ O\sqrt{E(f)} \frac{2mr}{\alpha} \sum_{k=-K}^{K} \left(\frac{2eT}{r}\right)^{m_k}.$$

Setting

$$\alpha = m\left(r \sum_{k=-K}^{K} \left(\frac{2eT}{r}\right)^{m_k}\right)^{2/3},$$

we have

$$\|a - b\| \leqslant O'\sqrt{m}\left(r \sum_{k=-K}^{K} \left(\frac{2eT}{r}\right)^{m_k}\right)^{1/3}, \tag{A.8}$$

where O' is a positive constant which only depends on signal f. We are now ready to estimate the error of the new algorithm Ψ_m.

$$|\Psi_m(t) - f(t)| \leqslant |\Psi_m(t) - \sum_{k=-K}^{K} \Phi_{m_k}(t) e^{-jtC_k}|$$
$$+ \left| \sum_{k=-K}^{K} \Phi_{m_k}(t) e^{-jtC_k} - f(t) \right|$$
$$\leqslant \left| \sum_{k=-K}^{K} \sum_{i=1}^{m_k} (a_{ki} - b_{ki}) \frac{\sin B_k(t - t_{ki})}{t - t_{ki}} e^{-jtC_k} \right|$$
$$+ \sum_{k=-K}^{K} |\Phi_{m_k}(t) - f_k(t)|.$$

By (A.5) and (A.8), for $t \in [-\tau, \tau]$ with $\tau \geqslant T$,

$$|\Psi_m(t) - f(t)| \leqslant O_1 mr\left(\sum_{k=-K}^{K} \left(\frac{2eT}{r}\right)^{m_k}\right)^{1/3}$$
$$+ O_2 r \sum_{k=-K}^{K} \left(\frac{2e\tau}{r}\right)^{m_k}.$$

When τ is significantly larger than T,

$$|\Psi_m(t) - f(t)| \leqslant Or \sum_{k=-K}^{K} \left(\frac{2e\tau}{r}\right)^{m_k},$$

where O is a constant which only depends on the signal f.

References

[1] M.G. Beaty and M.M. Dodson, "The distribution of sampling rates for signals with equally wide, equally spaced spectral bands", *SIAM J. Appl. Math.*, Vol. 53, June 1993, pp. 893–906.

[2] F.J. Beutler, "Error-free recovery of signals from irregularly spaced samples", *SIAM Rev.*, Vol. 8, July 1966, pp. 328–335.

[3] P.L. Butzer, W. Splettstösser and R.L. Stens,. "The sampling and linear prediction in signal analysis", *Jber. d. Dt. Math.-Verein.*, Vol. 90, 1988, pp. 1–70.

[4] J.A. Cadzow, "An extrapolation procedure for band-limited signals", *IEEE Trans. Acoust. Speech Signal Process.*, Vol. 27, February 1979, pp. 4–12.

[5] G. Calvagno and D.C. Munson Jr., "New results on Yen's approach to interpolation from nonuniformly spaced samples", *Proc. Internat. Conf. Acoust. Speech Signal Process.*, April 1990, pp. 1535–1538.

[6] D.S. Chen and J.P. Allebach, "Analysis of error in reconstruction of two-dimensional signals from irregularly spaced samples", *IEEE Trans. Acoust. Speech Signal Process.*, Vol. 35, February 1987, pp. 173–180.

[7] F.J.J. Clarke and J.R. Stockton, "Principles and theory of wattmeters operating on the basis of regularly sampled pairs", *J. Phys. E. Sci. Ints.*, Vol. 15, 1982.

[8] D. Del Re, "Bandpass signal filtering and reconstruction through minimum-sampling-rate digital processing", *Alta Frequenza*, Vol. XLVII, No. 9, September 1978.

[9] R.M. Fitzgerald and C.L. Byrne, "Extrapolation of band-limited signals: A tutorial", in: M. Kunt and F. Coulon, eds., *Signal Processing Theory and Application*, North-Holland, Amsterdam, 1980, pp. 175–179.

[10] J.D. Gaskell, *Linear Systems, Fourier Transforms, and Optics*, Wiley, New York, 1978.

[11] R.W. Gerchberg, "Super-resolution through error energy reduction", *Opt. Acta*, Vol. 21, No. 9, 1974, pp. 709–720.

[12] M. Golomb and H.F. Weinberger, "Optimal approximation and error bounds", in: R. Langer, ed., *On Numerical Approximation*, University of Wisconsin Press, Madison, WI, 1959, pp. 117–190.

[13] O.D. Grace and S.P. Pitt, "Quadrature sampling of high frequency waveforms", *J. Acoust. Soc. Amer.*, Vol. 44, 1968, pp. 1432–1436.

[14] N.E. Hurt, *Phase Retrieval and Zero Crossings*, Kluwer Academic Publishers, Boston, 1989.

[15] M.C. Jackson and P. Matthewson, "Digital processing of bandpass signals", *GEC J. Res.*, Vol. 4, No. 1, 1986.

[16] A.J. Jerri, "The Shannon sampling theorem – its various extensions and applications: A tutorial review", *Proc. IEEE*, Vol. 65, No. 11, November 1977.

[17] D.P. Kolba and T.W. Parks, "Optimal estimation for band-limited signals including time domain considerations", *IEEE Trans. Acoust. Speech Signal Process.*, Vol. 31, February 1983, pp. 113–122.

[18] M.A. Kowalski, "Optimal complexity recovery of band and energy-limited signals", *J. Complexity*, Vol. 2, 1986, pp. 239–254.

[19] H.J. Landau, "Extrapolating a band-limited function from its samples taken in a finite interval", *IEEE Trans. Inform. Theory*, Vol. IT-32, No. 4, July 1986.

[20] L. Levi, "Fitting a bandlimited signal to given points", *IEEE Trans. Inform. Theory*, Vol. 11, July 1966 pp. 372–376.

[21] C.A. Micchelli and T.J. Rivlin, "A survey optimal recovery", in: C.A. Micchelli and T.J. Rivlin, eds., *Optimal Estimation in Approximation Theory*, Plenum, New York, 1977.

[22] V.A. Morozov, "The error principle in the solution of operational equations by the regularization method", *USSR Compt. Math. Phys.*, Vol. 8, No. 2, 1968.

[23] D.H. Mugler, "Computationally efficient linear prediction from past samples of a band-limited signal and its derivatives", *IEEE Trans. Inform. Theory*, Vol. 36, 1990, pp. 589–596.

[24] D.H. Mugler and W. Splettstösser, "Difference methods for the prediction of band-limited signals", *SIAM J. Appl. Math.*, Vol. 46, 1986, pp. 930–941.

[25] M.Z. Nashed and G.G. Walter, "Generalized sampling theorems for functions in reproducing kernel Hiltert spaces", *Math. Control Signal Systems*, Vol. 4, 1991, pp. 363–390.

[26] A. Papoulis, "A new algorithm in spectral analysis and band-limited extrapolation", *IEEE Trans. Circuits Systems*, Vol. CAS-22, September 1975, pp. 735–742.

[27] L.C. Potter and K.S. Arun, "Energy concentration in band-limited extrapolation", *IEEE Trans. Acoust. Speech Signal Process.*, Vol. 37, July 1989, pp. 1027–1041.

[28] S. Ries, "Reconstruction of real and analytic band-pass signals from a finite number of samples", *Signal Processing*, Vol. 33, No. 3, September 1993, pp. 237–257.

[29] J.L.C. Sanz and T.S. Huang, "Some aspects of band-limited signal extrapolation: Models, discrete approximations and noises", *IEEE Trans. Acoust. Speech Signal Process.*, Vol. 31, No. 6, December 1983.

[30] H.J. Schlebusch and W. Splettstösser, "On a conjecture of J.L.C. Sanz and T.S. Huang", *IEEE Trans. Acoust. Speech Signal Process.*, Vol. 33, October 1985.

[31] D. Slepian, "Prolate spheroidal wave functions, Fourier analysis, and uncertainty – V. The discrete case", *Bell Systems Technol. J.*, Vol. 57, May–June 1978, pp. 1371–1430.

[32] D. Slepian, H.O. Pollak and H.J. Landau, "Prolate spheroidal wave functions I, II", *Bell Systems Technol. J.*, Vol. 40, January 1961, pp. 43–84.

[33] A.N. Tikhonov and V.Y. Arsenin, *Solutions of Ill-Posed Problems*, Winston, Washington, DC, 1977.

[34] R.G. Vaughan, N.L. Scott and D.R. White, "The theory of bandpass sampling", *IEEE Trans. Signal Process.*, Vol. 39, September 1991, pp. 1973–1984.

[35] W.M. Waters and B.R. Jarrett, "Bandpass signal sampling and coherent detection", *IEEE Trans. Aerospace Electron. Systems*, Vol. AES-18, No. 4, November 1982.

[36] X.-G. Xia, Z. Zhang and C. Lo, "Error analysis of the MMSE estimator for multidimensional band-limited extrapolations from finite samples", *Signal Processing*, Vol. 36, No. 1, 1994, pp. 55–69.

[37] W.Y. Xu and C. Chamzas, "On the extrapolation of band-limited functions with energy constraints", *IEEE Trans. Acoust. Speech Signal Process.*, Vol. 31, No. 5, October 1983.

[38] J.L. Yen, "On nonuniform sampling of bandlimited signals", *IRE Trans. Circuit Theory*, Vol. 3, December 1956, pp. 251–257.

[39] D.C. Youla, "Generalized image restoration by the method of alternating orthogonal projections", *IEEE Trans. Circuits Systems*, Vol. CAS-25, September 1978, pp. 694–701.

[40] X.W. Zhou and X.-G. Xia, "The extrapolations of high dimensional band-limited signals", *IEEE Trans. Acoust. Speech Signal Process.*, Vol. 37, October 1989.